Topological Analysis of the Experimental Electron Densities of Small Organic Molecules, Part 2[+]

Topological Analysis of the Experimental Electron Density of Diisocyanomethane at 115 K

Tibor Koritsánszky,[b] Jürgen Buschmann,[a] Dieter Lentz,[c] Peter Luger,*[a] Genivaldo Perpetuo,[a] and Matthias Röttger[c]

Abstract: The structure and charge density of diisocyanomethane, derived from low-temperature X-ray diffraction data and by ab initio calculations are reported. Different refinement models are tested to judge the physical significance of the density parametrization. The experimental distances of the formal triple bonds are significantly shorter than those obtained by energy optimization. In terms of topological indices the former method gives a higher bond order than the latter one, even if the calculation is performed at the experimental geometry, indicating that crystal field effects may not be negligible when the results are compared. These effects, although caused by weak close contacts, can directly be revealed by comparing the electrostatic potential extracted from the diffraction data with that derived from the wave function of the isolated molecule.

Keywords: ab initio calculations · bond-topological indices · electronic structure · electrostatic potential · multipole refinement

Introduction

The first isocyanides, ethyl isocyanide and phenyl isocyanide, were prepared more than a hundred years ago by Gautier[1] and Hofmann.[2] Due to their extremely bad odor and limited synthetic routes the chemistry of the less stable isomers of the nitriles remained unexplored for a long time. Since Ugi's discovery of an efficient synthesis from the corresponding formamides, isocyanides have been used more and more as building blocks in organic syntheses.[3] The coordination chemistry of the isocyanide ligands was strongly influenced by the work of Malatesta, Bonati, and others,[4–10] and it was recognized that the ligand properties of the isocyanide group can easily be tuned by the electronic properties of the substituent; the ligands range from good σ-donor ligands to extremely strong π-accepting ligands such as trifluoromethyl isocyanide.[11]

During recent years a number of small isocyanides such as CN–CN,[12–14] CN–NC,[15] NC–CC–NC,[16, 17] H–CC–NC,[18–21] $H_2C(CN)(NC)$,[22–25] and $H_2C(NC)_2$[26, 27] have been prepared and characterized by various methods. Nevertheless, the number of structurally characterized small isocyanides is still limited (Table 1), and the number of those investigated by X-ray crystallography is even smaller. Since the bonding situation in this type of compounds is peculiar due to the presence of a formally divalent carbon atom with a coordination number of only one, an experimental charge density determination of an isocyanide is of interest.

Apart from the experimental difficulties arising from the thermal instability of diisocyanomethane, which violently decomposes on warming above 0 °C, the compound is an ideal candidate for an experimental charge density study, as it is a rather small structure, crystallizing in a centrosymmetric space group ($P2_1/n$) with one molecule in the asymmetric unit.

Experimental electron density studies are becoming increasingly important.[37] Recent advances of X-ray diffraction techniques make it possible to obtain high-resolution diffraction patterns and thus a detailed mapping of the charge distribution within the time interval needed for the corre-

[a] Prof. Dr. P. Luger, Dr. J. Buschmann, Dr. G. Perpetuo
Institut für Chemie, Abteilung Kristallographie der Freien Universität
Takustrasse 6, D-14195 Berlin (Germany)
Fax: (+49)30 8383464
E-mail: luger@chemie.fu-berlin.de

[b] Prof. Dr. T. Koritsánszky
Department of Chemistry
University of the Witwatersrand
WITS 2050, Johannesburg (South Africa)

[c] Prof. Dr. D. Lentz, Dr. M. Röttger
Institut für Chemie, Abteilung Anorganische und Analytische Chemie,
der Freien Universität
Fabeckstrasse 34–36, D-14195 Berlin (Germany)

[+] Part 1 see ref. [41].

  0947-6539/99/0511-3413 $ 17.50+.50/0

Table 1. C–NC and CN–C bond lengths in isocyanides [Å].

Isocyanide	r(C–NC)	r(CN–C)	Phase	Reference
H_3C–NC	1.428(2)	1.166(1)	gaseous	[28]
F_3C–NC	1.407	1.171(3)	gaseous	[29]
F_3C–CH_2–NC	1.424(2)	1.145(2)	solid	[30]
H–NC		1.172	gaseous	[31]
$H_2C(CN)(NC)$	1.43(2)	1.16(2)	solid	[25]
	1.40(2)	1.18(2)		
$H_2C(NC)_2$	1.427(1)	1.155(1)	solid	[27]
	1.425(1)	1.151(1)		
H_5C_6–NC	1.410	1.142	gaseous	[32]
F_5C_6–NC	1.380(2)	1.159(3)	solid	[33]
F_2C=CF–NC	1.372(1)	1.168(2)	solid	[34]
H_2C=CH–NC	1.379(6)	1.174(6)	gaseous	[35]
NC–NC	1.316(3)	1.175(2)	gaseous	[36]
HCC–NC	1.317(1)	1.175(1)	gaseous	[21]
NC–CC–NC	1.306(1)	1.178(1)	gaseous	[17]

sponding quantum-chemical calculations.[38] Routine applications of the method can lead to ambiguous results on account of the relatively complicated nature of the modeling procedure involved. In the analysis of the adequacy of the density models applied chemical preconceptions and physical restrictions play an important role. Recent studies that studied the total, rather than the deformation density,[39-41] emphasize the importance of the finding that the experimentally determined density, characteristic of the crystalline state, has basically the same topology as that calculated from the ground-state wave function of the corresponding isolated molecule. These results suggest that one should analyze deviations in fine topological details of the densities obtained by the two methods in order to learn about the nature of the intermolecular interactions that stabilize the crystal and/or to resolve model indeterminacies, if the deviations considered cannot be attributed directly to crystal field effects. To explore these aspects topological analyses of the experimental charge density of small molecules[41, 42] are reported.

Density models and multipole refinements

The atomic positions and displacement amplitudes from reference [27] were used as starting parameters in the multipole refinements based on the Hansen–Coppens formalism[43] and carried out with the full-matrix least-squares program (XDLSM) of the XD program package.[44] The quantity $\Sigma_{\mathbf{H}} w_{\mathbf{H}}$ $(|F_{obs}(H)| - k|F_{cal}(H)|)^2$ was minimized by using the statistical weight $w_{\mathbf{H}} = [\sigma(F_{obs}(H))]^{-2}$ and only those structure factors which met the criterion of $F_{obs}(H) > 3\sigma(F_{obs}(H))$. The following conditions were common to all refinement models applied. The core and the spherical valence densities were composed of Hartree–Fock wave functions expanded over Slater type basis functions.[45] For the deformation terms single-zeta orbitals with energy-optimized Slater exponents were taken and kept fixed.[45] The scattering factor curve of the hydrogen atoms was calculated from contracted radial density functions ($\kappa = 1.2$), which provide a simple analytical approximation to the scattering factor introduced by Stewart et al.[46] The level of the expansion was hexadecapolar and dipolar for the heavy and for the hydrogen atoms, respectively. A bond-directed quadrupole ($l = 2, m = 0$) was also introduced for the hydrogen atoms. The molecule was kept neutral during all refinements.

The atomic numbering used is shown in Figure 1, while the definition of the atomic site coordinate systems is contained in the Supporting Information. Several refinement models were

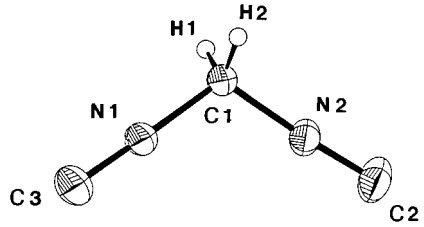

Figure 1. ORTEP[47] representation of the diisocyanomethane molecule at 50% probability level.

tested, differing in the extent to which symmetry was imposed on the static density. In the first model m1, beside the conventional parameters, all density parameters described above, including different radial screening parameters (κ values) for the carbon and nitrogen atoms, were fitted against the data. The thermal motion of the hydrogen atoms was described at the isotropic level. In model m2 the local C_{2v} symmetry of the atom C1 was implemented; the same symmetry (C_{2v}) was applied to the whole molecule and introduced by application of chemical constraints between the two hydrogen atoms and the two NC groups. In addition, the deformation density of the NC group was forced to possess rotational symmetry, that is only $P_{l,m=0}$ population parameters were allowed for the C2 and N2 (C3 and N1) atoms. To reduce indeterminacies due to vibrational smearing, the procedure applied in the charge density study of aspartic acid[42] was followed in refinement m3 by using the mean-square displacement amplitudes (MSDAs) calculated from the ab initio (HF/6-311^{++}G(d,p)) harmonic force field of the isolated, optimized molecule as starting parameters. The MSDA tensors corresponding to the internal vibrational modes (U_{int}) were transformed from the inertial system of the optimized molecule to the crystal system. In the course of subsequent refinements the shifts in the displacement parameters were restricted by rigid-link type constraints[48] to fulfill the rigid-body motion requirement. This was achieved by invoking $6N - 20$ ($N = 7$ is the number of atoms) independent rigid-link constraints, that is by keeping the MSDAs along links equal for a necessary number of atom pairs ($\Delta\text{MSDA} = 0$).[49] The full set of independent rigid-link constraints corresponds to a fit of the $\boldsymbol{T}$, $\boldsymbol{L}$, and $\boldsymbol{S}$ tensors of the rigid-body motion model[50] to the structure factors, giving rise to MSDAs for which $U = U_{TLS} + U_{int}$. During this step the C–H distances were kept at values obtained by the geometry optimization. The statistical figures of merit of the different refinements are given in Table 2. The multipole parameters based on model m3 and the related atomic fractional coordinates and displacement parameters are in the Supporting Information.

0947-6539/99/0511-3414 $ 17.50+.50/0 *Chem. Eur. J.* **1999**, *5*, No. 11

Table 2. Figures of merit of the different refinement models.

	Spherical model	Aspherical models		
		m1	m2	m3
NREF	1635	1635	1635	1635
NVAR	48	177	71	60
NREF/NVAR	34	9	23	27
$R(F)$	0.0577	0.0340	0.0344	0.0353
$R_w(F)$	0.0504	0.0239	0.0289	0.0295
GOF	5.44	2.70	3.15	3.19
$(\Delta/\sigma)_{max}$	3.1×10^{-3}	4.3×10^{-2}	7.9×10^{-4}	7.7×10^{-5}

Theoretical calculations

Ab initio calculations were performed with the Gaussian94 program package[51] at the Hartree-Fock (HF) and MP2 levels of theory. Full optimizations with the C_{2v} symmetry of the molecule were carried out with the 6-311^{++}G(3d,3p) basis sets starting from the X-ray structural data. As convergence criteria the default threshold limits of 0.00045 and 0.0018 au were applied for the maximum force and displacement, respectively. The optimizations were followed by the evaluation of the harmonic vibration frequencies (HF) and amplitudes. The topological analyses (AIMPACK[52]) were based on the wave functions obtained by single point calculations using the experimental geometry to allow direct comparison with the topological indices obtained experimentally. The theoretical deformation electron density and the Laplacian map, however, were calculated with the optimized geometry.

Results and Discussion

From the statistical figures (Table 2) of different refinements it is evident that the most restricted model (m3) fits the data as well as model m2. Although the unconstrained model (m1) has the lowest residuals, its performance is doubtful considering the 106 and 117 additional variables compared to models m2 and m3, respectively. The ratio of observations-to-variables increases by a factor of three for the most constrained model relative to the unrestricted one. Based on the final shift-to-error ratios of refined parameters, the convergence achieved is the best for model m3. This is accompanied by a decreasing correlation among the parameter estimates as going from the less to the more constrained model. The usefulness of the different constraints applied is also justified by comparative analyses of the residual densities. In Table 3 the experimental internuclear distances are compared to those obtained by optimization. The theoretical values, especially for the formal triple bonds, are higher than the experimental ones except for the C–N single bonds given by the spherical-atom model. It is to be noted that there are differences in the internuclear distances in the range of three times their standard uncertainties, obtained by refinements m1 and m2. The symmetry imposed on the density inverts the order of the distances obtained by the unconstrained refinement. The C1–N1/C1–N2 bond lengths become slightly longer/shorter, while for the triple bond the opposite trend is observed. This can be interpreted as shifts of the N1/N2 nitrogen atoms toward the C3/C1 carbon atoms. No significant changes in the geometry are observed in connection with the rigid-link constraints. The C-N-C moiety is almost linear with bond angles of 176.1(1) and 177.8(1)°; the N-C-N bond angle is 110.6(1)°. The analysis of the Δ MSDA values shows that the displacement amplitudes are considerably biased by model m1, especially those assigned to the atoms forming the isocyanide bond (Table 4). This is also seen, although to a lesser extent, in the anisotropic displacement amplitudes of model m2. The deviations from the physically acceptable values are also pronounced for the nonbonded links. The corresponding values for the C–N bonds obtained by models m1 and m2 show a similar trend as that found for the internuclear distances.

Table 3. Experimental and optimized bond lengths [Å].

Bond	Experimental spherical	m1	m2	m3	Theoretical MP2/6–311^{++} G(3d,3p)
C1–N1	1.4326(11)	1.4116(13)	1.4148(13)	1.4161(11)	1.4205
C1–N2	1.4223(15)	1.4177(15)	1.4137(13)	1.4146(12)	
N1–C3	1.1432(12)	1.1624(11)	1.1588(11)	1.1585(11)	1.1870
N2–C2	1.1541(15)	1.1572(15)	1.1640(13)	1.1641(13)	
C1–H	fixed at theoretical value				1.092

Table 4. Difference mean-square displacement amplitudes Δ_{ik}[10^4 Å^2].

Bonds	Spherical	m1	m2	m3	HF/6–311^{++}G(3d,3p)
C1–N1	–35	–1	11	4	4
C1–N2	–38	13	1	4	4
N1–C3	38	5	11	3	3
N2–C2	4	11	5	3	3
C1–H1	48	48	48	48	49
C1–H2	48	48	48	48	49
Links					
N1 ··· N2	8	–12	–2	0	0
N1 ··· C2	19	3	3	2	3
N1 ··· H1	80	80	80	80	79
N1 ··· H2	78	78	78	78	79
N2 ··· C3	43	15	14	2	3
N2 ··· H1	78	78	78	78	79
N2 ··· H2	80	80	80	80	79
C1 ··· C2	44	–3	4	–1	–1
C1 ··· C3	73	7	0	–1	–1
C2 ··· C3	29	2	8	–1	0
C2 ··· H1	93	93	93	93	93
C2 ··· H2	94	94	94	94	93
C3 ··· H1	95	95	95	95	93
C3 ··· H2	95	95	95	95	93
H1 ··· H2	0	0	0	0	0

Figure 2 compares the experimental (m1, m3) and the theoretical deformation electron density in the molecular plane. The striking difference is that the interatomic regions are richer in electron density in the former map than in the latter. The experimentally found extra charge accumulation in the terminal N–C bond appears to be at the expense of charge in the nonbonded region of the carbon atom. This is accompanied by a shift of the bond peak towards the terminal carbon atom. In the theoretical map this peak is localized midway between the atoms. The deformation density corresponding to refinement m1 shows minor asymmetry in terms of the chemically equivalent bonds as well as of the lone-pair

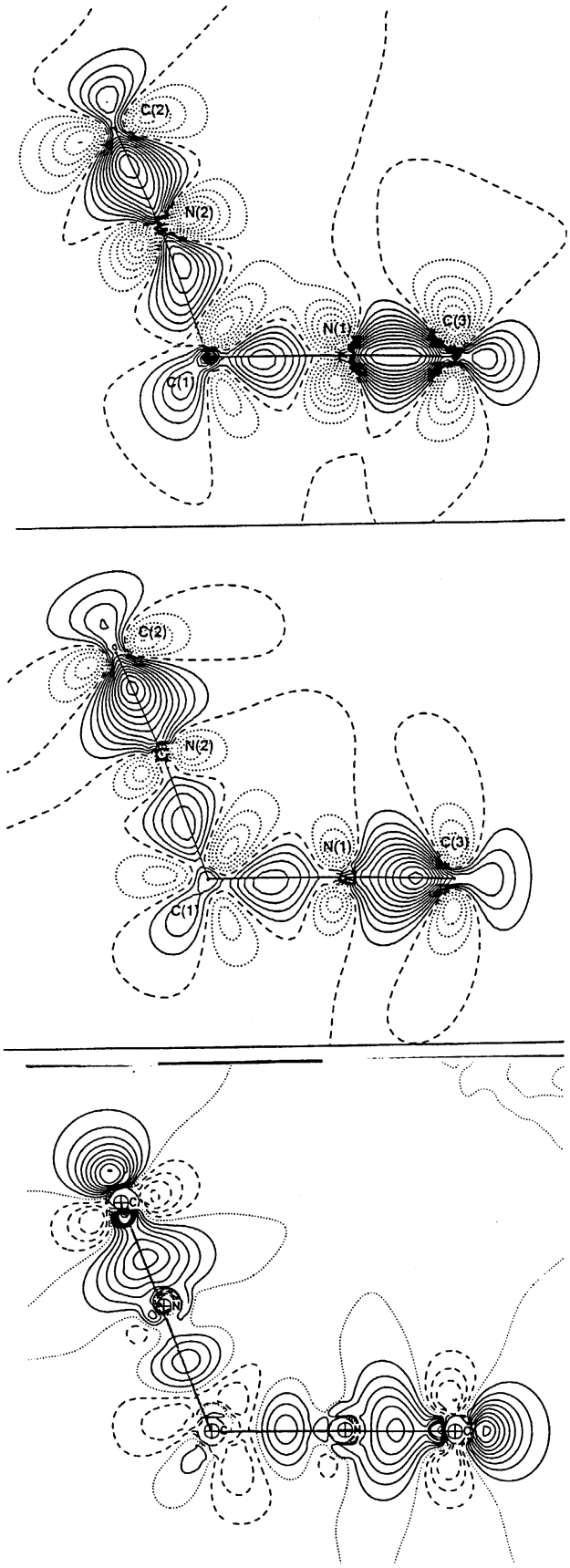

Figure 2. Deformation electron density of diisocyanomethane in the molecular plane, top: from experimental data, model m1; middle: from experimental data, model m3; bottom: theoretical model calculated at HF/6–311^{++}G(d,p) level. Contour intervals 0.1 e Å^{-3}.

peaks. The comparison of the Laplacian functions obtained by the two different methods (Figure 3) also reveals significant differences in line with the findings described above. The bonded valence shell charge concentrations (VSCCs) appear to be more pronounced in the experimental relief maps than

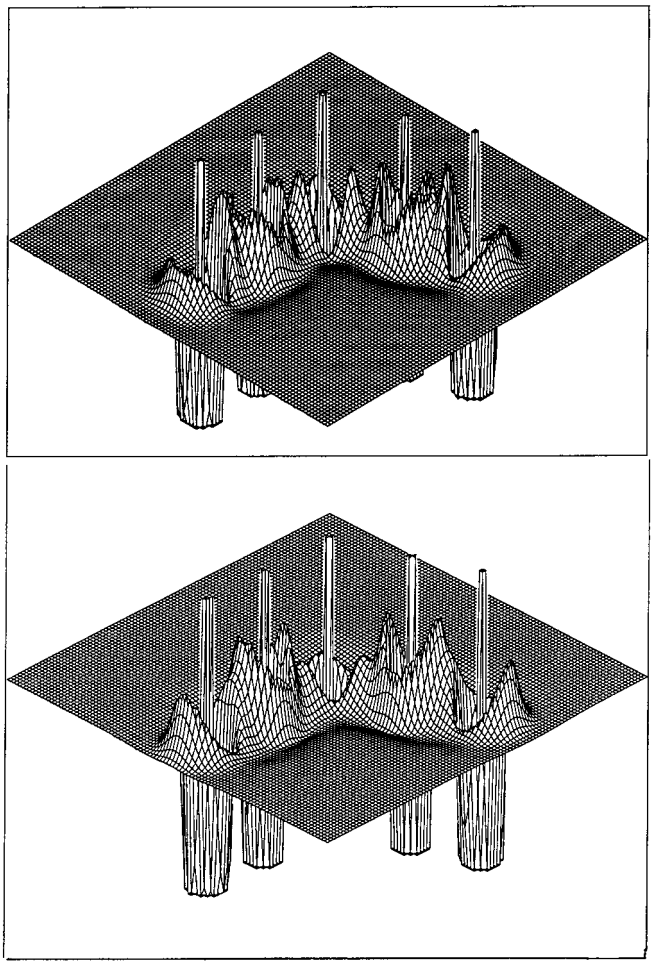

Figure 3. Relief representation of the negative Laplacian function in the main plane of the diisocyanomethane molecule, cut-off value ± 80 e Å^{-5}; top: experimental, model m3; bottom: theoretical model calculated at MP2/6–311^{++}G(d,p) level.

those exhibited by the calculated function. The theory does not reproduce the experimentally found bonded VSCC of the terminal carbon atom. This VSCC is the sharpest peak on the experimental map. On the other hand, the nonbonded VSCCs are almost equally developed.

The result of the quantitative analysis of the densities is shown in Table 5 in terms of bond topological parameters,[53] such as the locations of the bond critical points (CP, located at $\mathbf{r}_b$ where $\nabla\rho(\mathbf{r}_b) = 0$), the values of $\rho(\mathbf{r}_b)$ and its Laplacian ($\nabla^2\rho(\mathbf{r}_b)$, and the bond ellipticities εs (a measure of the deviation of the negative principal curvatures at the bond CP). The comparison of the $\rho(\mathbf{r}_b)$ values, regardless of the refinement model considered, also reveals the experimentally found extra charge accumulations in the C–N bonds. The other topological indices derived from the experimental density show considerable model dependence. In terms of

0947-6539/99/0511-3416 $ 17.50+.50/0 *Chem. Eur. J.* **1999**, *5*, No. 11

Table 5. Bond topological parameters of diisocyanomethane, ε: ellipticity of the density peak at the bond critical point, d: distance of the bond critical point from atom 1.

Bond atom1 – atom2	ρ [Å^{-3}]	$\nabla^2\rho$ [Å^{-5}]	ε	d [Å]	Method
C1–N1	1.83	– 17.9	0.14	0.634	MP2/6 – 311^{++}G(3d,3p)
C1–N1	2.13(4)	– 21.4(2)	0.14	0.659	m1
C1–N1	2.07(4)	– 22.2(2)	0.05	0.630	m2
C1–N1	2.03(3)	– 20.6(2)	0.08	0.629	m3
C1–N2	1.82	– 17.9	0.14	0.635	MP2/6 – 311^{++}G(3d,3p)
C1–N2	1.97(7)	– 31.4(4)	0.13	0.527	m1
C1–N2	2.07(6)	– 22.3(2)	0.05	0.629	m2
C1–N2	2.04(3)	– 20.7(2)	0.08	0.628	m3
C3–N1	3.00	– 11.3	0.02	0.484	MP2/6 – 311^{++}G(3d,3p)
C3–N1	3.52(14)	– 40.1(9)	0.39	0.415	m1
C3–N1	3.39(7)	– 39.8(1)	0.0	0.417	m2
C3–N1	3.47(5)	– 48.8(1)	0.0	0.428	m3
C2–N2	3.00	– 11.3	0.02	0.484	MP2/6 – 311^{++}G(3d,3p)
C2–N2	3.43(14)	– 47.0(9)	0.11	0.429	m1
C2–N2	3.37(7)	– 41.0(1)	0.0	0.420	m2
C2–N2	3.44(5)	– 49.9(1)	0.0	0.433	m3
C1–H1	1.97	– 26.0	0.02	0.755	MP2/6 – 311^{++}G(3d,3p)
C1–H1	1.84(6)	– 20.7(3)	0.07	0.795	m1
C1–H1	1.82(6)	– 20.3(2)	0.15	0.756	m2
C1–H1	1.83(4)	– 20.9(1)	0.11	0.759	m3
C1–H2	1.97	– 26.0	0.02	0.755	MP2/6 – 311^{++}G(3d,3p)
C1–H2	1.79(5)	– 21.4(1)	0.21	0.771	m1
C1–H2	1.82(4)	– 20.4(1)	0.15	0.755	m2
C1–H2	1.83(4)	– 21.0(1)	0.11	0.758	m3

the $\nabla^2\rho(\mathbf{r}_b)$ values, model m1 gives higher charge accumulations in the C1–N2 than in the C1–N1 bond. This is most likely due to the different locations of the bond CPs. In the former bond the CP is located 0.13 Å closer to the C1 atom than in the latter one. Similarly, the Laplacian is more negative in the C2–N2 than in the C3–N1 bond. In the latter case an unrealistically high value for the ellipticity is obtained. An important observation is that the $\nabla^2\rho(\mathbf{r}_b)$ values for the triple bonds obtained by model m3 are markedly higher than the corresponding values by model m2. Table 6 contains bond

Table 6. Experimental bond topological parameters for C···H close contacts.[a]

C···H	Symmetry operation	R(C···H) [Å]	ρ [Å^{-3}]	$\nabla^2\rho$ [Å^{-5}]	R(C–CP) [Å]
C2···H1	$1/2+x$, $3/2-y$, $1/2+z$	2.7668(7)	0.04(1)	0.44(2)	1.6841
C2···H2	$1/2-x$, $1/2+y$, $3/2-z$	2.6708(9)	0.05(1)	0.6(2)	1.5969
C3···H1	$3/2+x$, $3/2-y$, $-1/2+z$	2.5878(9)	0.05(1)	0.7(2)	1.6107
C3···H2	$1/2-x$, $1/2+y$, $1/2-z$	2.7271(10)	0.05(1)	0.6(2)	1.6315

[a] R(C···H) and R(C–CP) are the distances of the carbon atom from the hydrogen atom and from the CP of the C···H interaction.

topological indices for the strongest nonbonded interactions. (3, – 1) CPs were found between the terminal carbon and the hydrogen atoms of the neighboring molecules. For all of these close contacts the density is low and the Laplacian is positive at the bond CP, indicating closed-shell interactions.

Figure 4 compares the experimental with the theoretical electrostatic potential by three-dimensional iso-potential surfaces. The former function which was derived from multipole parameters according to the method of Su and Coppens[54] and which corresponds to the density extracted from the crystal, exhibits more extended negative (red) surfaces for the chosen potential value than that calculated from the wave function of the isolated molecule. The polarization shown along the H-C-N-C framework can be interpreted as the effect of intermolecular electrostatic interactions manifested in short C···H contacts.

Figure 4. Three-dimensional color view of the electrostatic potential of the diisocyanomethane molecule; three isopotential surfaces, blue 0.5, red – 0.3, net 0.0 e Å^{-1}; top: experimental, molecule in crystal; bottom: theoretical, isolated molecule, calculated at HF/6 – 311^{++}G(3df,3pd) level.

Conclusion

This study demonstrates the importance of the careful interpretation of X-ray data, if precise estimates of positional, thermal, and density parameters are to be extracted. The estimates of internuclear distances and displacement amplitudes are evidently biased by the spherical atom model. One should be able to check this by comparing the results with those obtained with more sophisticated density models. Indeed, the "asphericity" shift of the N1 atom, that is its migration toward the C3 atom to account for a part of the density in the triple bond, is in line with the expectation. The C1–N2 and N2–C2 bond lengths obtained by the spherical atom model are, however, statistically equal to those given by

the unrestricted multipole refinement. The latter bond even passes Hirshfeld's rigid-bond test. To this geometrical asymmetry, although it can be considered as highly significant in terms of standard uncertanties, no chemical relevance should be attributed.

The multipole model m1 shifts the atoms toward a "more symmetric" molecule. This geometrical change can formally be described by displacements of both nitrogen atoms toward the C1 atom, which make the triple and single bond lengths longer and shorter, respectively. The chemically equivalent bonds remain significantly different, but the order of the distances established by the conventional model is not preserved. Whether this is a genuine improvement in the parameter estimates or not, remains a question, although the lengthening of the triple bonds can be interpreted as the effect of the C···H interactions. The C3–N1 bond length is longer than the C2–N2 one, which is also in line with the C···H contacts being stronger (shorter) at the former than at the latter site. The corresponding density shows departures from the symmetry characteristic of the isolated molecule, especially if it is interpreted in terms of the deformation density map. The topological indices also show considerable asymmetry, mainly in the single bonds where the CP locations are markedly different.

The symmetry-constrained density model (m2), although it results in a structure that is even closer to the symmetric one, preserves the order of the formal triple bonds given by model m1. An important observation is that the geometrical equivalence of the single bonds is now accompanied by the topological equivalence of their densities. This self-consistency suggests the restricted model to be superior to the unrestricted one. The latter, being overparametrized, is more likely to absorb noise or systematic errors in the data than the former one.

The results obtained by the two aspherical atom refinements appear to be precise, but the comparison reveals inaccuracy. In other words, the most accurate structure one can extract from the given data set at the given level of sophistication of the density model seems to be somewhere between those obtained in refinements m1 and m2, that is a symmetric one. The same argument applies with respect to the displacement amplitudes. Both aspherical atom models reduce the difference in the bond projected MSDAs, compared to those of the spherical atom model, but the comparison of the individual MSDA values may not bear physical relevance. Nevertheless, the introduction of the rigid-link constraints (m3) which imposes changes in the displacement amplitudes (changes which are not significant in statistical terms but do possess physical significance), leads to changes in fine details of the topology of the static density without any shift in atomic positions. The reduced bias in the displacement amplitudes resulted in considerable changes in the Laplacian and in an overall enhancement of the VSCCs. This demonstrates that the deconvolution of the vibrational motion has limited success, even if an aspherical model is applied in the interpretation of the data. The well-established physical evidence embedded in the rigid-bond constraints certainly helps evaluate the adequacy of the density model and the accuracy of the parameter estimates.

With respect to the chemical relevance of this study the following can be stated. Normally the bonding in isocyanides is described by the two resonance forms A and B (Scheme 1). As the N≡C bond length in isocyanides is much shorter than an N=C bond length and only slightly longer than the C≡N bond length in nitriles, one expects the resonance form B to possess a greater weight, suggesting a charge flow from the

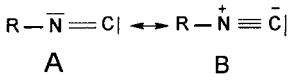

Scheme 1.

nitrogen to the carbon atom. The topology of the experimental density supports this argument in terms of the sharp bonded VSCCs of the terminal carbon atoms. In all C–N bonds the Laplacian based on the X-ray data, independent of the restrictions applied in the different refinement models, indicates more charge concentrations than that based on the wave function. The same tendency is shown in the values of the density at the bond critical points.

Last but not least, quite strong indications were found for the effect of the crystal field on the topology of the density. The intermolecular interactions in question, being of electrostatic nature, are rather expected to polarize the density than to induce direct changes in the molecular geometry. This can be best seen in the electrostatic potential. It is evident that even very week interactions should be considered, when experimental and theoretical results are compared.

Experimental Section

Diisocyanomethane, the so far only known geminal diisocyanide, was prepared from bis(formamido)methane by Ugi synthesis (Scheme 2) and purified by fractional condensation under vacuum. The colorless crystalline material was collected in a trap kept at $-30\,^{\circ}C$. It melted at $-15\,^{\circ}C$ to give a colorless liquid which rapidly turned brown due to decomposition. This

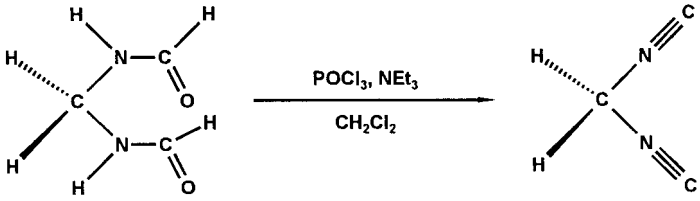

Scheme 2.

exothermic decomposition reaction became vigorous above $-10\,^{\circ}C$. To avoid explosion the compound should be prepared only in small amounts. By slowly cooling the solution of diisocyanomethane in diethyl ether/pentane from -20 to $-90\,^{\circ}C$ over a period of several days it was possible to grow single crystals. They were inspected and one was prepared under a cold N_2 gas stream.[18–21] The prepared crystal was transferred to the cold N_2 gas stream of the diffractometer[55] and slowly cooled down further to $-155\,^{\circ}C$; the crystal did not show indications of phase transition.

Diisocyanomethane crystallizes in the monoclinic space group $P2_1/n$, with lattice constants similar to those found for the isomeric cyanoisocyanomethane[25] (Pn) and malononitrile (dicyanomethane)[56, 57] ($P2_1/n$). The X-ray reflections had smooth profiles with widths, however, of up to 2° by ω scans. All profiles were recorded. The orientation matrix and lattice

0947-6539/99/0511-3418 $ 17.50+.50/0 Chem. Eur. J. 1999, 5, No. 11

constants were determined from 34 reflections with $21.5^\circ \le 2\theta \le 39.1^\circ$. Reflections from a bit more than a half sphere in reciprocal space were measured. After data reduction, 48.5% of the reflections measured had F^2_{obs} values above $2\sigma(F^2_{obs})$. The check reflections showed a continuous drop of 6% during the two-week long measurement. Therefore, the reflection intensities were scaled according to the change in the check reflections. This was followed by a correction for Lorentz and polarization effects. Crystal data and further details of the measurement are given in Table 7. Crystallographic data (excluding structure factors) for the structure reported in this paper (with multiple local coordinate systems and the refined multiple parameters) have been deposited with the Cambridge Crystallographic Data Centre as supplementary publication no. CCDC-120952. Copies of the data can be obtained free of charge on application to CCDC, 12 Union Road, Cambridge CB2 1EZ, UK (fax: (+44) 1223-336-033; e-mail: deposit@ccdc.cam.ac.uk).

Table 7. Crystal data and experimental conditions.

empirical formula	$C_3H_2N_2$
formula weight	66.07 g mol^{-1}
temperature	$-155(2)^\circ$C
radiation	
$Mo_{K\alpha}$, Nb filter	
wavelength	0.71068 Å
crystal system	monoclinic
space group	$P2_1/n$
unit cell dimensions	
a [Å]	6.278(2)
b [Å]	7.672(2)
c [Å]	7.978(2)
β [°]	99.91(3)
volume [Å^3]	378.5(2)
Z	4
ρ_{calcd}[g cm^{-3}]	1.159
μ [mm^{-1}]	0.079
$F(000)$	136
crystal size	$0.68 \times 0.60 \times 0.38$ mm
θ range for data collection	3.7 to 50.0 °
$((\sin\theta)/\lambda)_{max}$	1.08 Å^{-1}
index ranges	$-11 \le h \le 11$, $-14 \le k \le 7$, $-14 \le l \le 14$
scan method, steps	ω-2θ, 0.03–0.06 °
scan width	$\Delta\omega = 2.19^\circ + 0.52^\circ \tan\omega$
scan rate (ω) to reach $I/\sigma(I) > 100$ within the rate interval	0.6–2.4° min^{-1}
reference reflections	2 −3 −2, 3 1 −1, 0 −1 6
reflections collected	7769
independent reflections	3617 ($R_{int} = 0.0395$)

Acknowledgements

This work was supported by the Deutsche Forschungsgemeinschaft (grant number Lu 222/18) and the Fonds der Chemischen Industrie.

[1] A. Gautier, *Justus Liebigs Ann. Chem.* **1867**, *142*, 289; *Justus Liebigs Ann. Chem.* **1868**, *146*, 124.
[2] A. W. Hofmann, *Justus Liebigs Ann. Chem.* **1867**, *144*, 114; *ibid.* **1868**, *146*, 107.
[3] I. Ugi, *Angew. Chem.* **1982**, *94*, 826; *Angew. Chem. Int. Ed. Engl.* **1982**, *21*, 810; *Isonitrile Chemistry*, (Ed.: I. Ugi), Academic Press, New York **1971**.
[4] L. Malatesta, F. Bonati, *Isocyanide Complexes of Metals*, Wiley, London **1969**.
[5] P. M. Treichel, *Adv. Organomet. Chem.* **1973**, *11*, 21.
[6] F. Bonati, G. Minghetti, *Inorg. Chem. Acta* **1974**, *9*, 95.
[7] Y. Yamamoto, *Coord. Chem. Rev.* **1980**, *32*, 193.
[8] E. Singleton, H. E. Oosthuizen, *Adv. Organomet. Chem.* **1983**, *22*, 209.
[9] P. Fehlhammer, *Nachr. Chem. Lab. Techn.* **1982**, *30*, 187.
[10] F. E. Hahn, *Angew. Chem.* **1993**, *105*, 681; *Angew. Chem. Int. Ed. Engl.* **1993**, *32*, 650.
[11] D. Lentz, *Angew.Chem.* **1994**, *106*, 1377; *Angew. Chem. Int. Ed. Engl.* **1994**, *33*, 1315.
[12] T. van der Does, F. Bickelhaupt, *Angew. Chem.* **1988**, *100*, 998; *Angew. Chem. Int. Ed. Engl.* **1988**, *27*, 936 (given by mistake as CN−NC).
[13] F. Stroh, M. Winnewisser, *Chem. Phys. Lett.* **1989**, *155*, 21.
[14] F. Stroh, M. Winnewisser, H. P. Reisenauer, G. Maier, S. J. Goede, F. Bickelhaupt, *Chem. Phys. Lett.* **1989**, *160*, 105.
[15] G. Maier, H. P. Reisennauer, J. Eckwert, C. Sierakowski, T. Stumpf, *Angew. Chem.* **1992**, *104*, 1287; *Angew. Chem. Int. Ed. Engl.* **1992**, *31*, 1218.
[16] A. M. Smith, G. Schallmoser, A. Thoma, V. E. Bondybey, *J.Chem. Phys.* **1993**, *98*, 1776.
[17] C. Bartel, P. Botschwina, H. Bürger, A. Guarnieri, Ä. Heyl, A. Huckauf, D. Lentz, T. Merzliak, El B. Mkadmi, Angew. Chem. **1998**, *110*, 3036; *Angew. Chem. Int. Ed. Engl.* **1998**, *37*, 2879.
[18] M. Krüger, H. Dreizler, D. Preugschat, D. Lentz, *Angew. Chem.* **1991**, *103*, 1674; *Angew. Chem. Int. Ed. Engl.* **1991**, *30*, 1644.
[19] L. Zanathy, H. Bock, D. Lentz, D. Preugschat, P. Botschwina, *J. Chem. Soc. Chem. Comm.* **1992**, 403.
[20] A. Guarnieri, R. Hinze, M. Krüger, H. Zerbe-Foese, D. Lentz, D. Preugschat, *J. Mol. Spectrosc.* **1992**, *156*, 39.
[21] H. Bürger, S. Sommer, D. Lentz, D. Preugschat, *J. Mol. Spectrosc.* **1992**, *156*, 360.
[22] G. D. Hartmann (Merck), US-A 4021 438, *Chem. Abstr.* **1977**, *87*, 53264s.
[23] W. Liebenow, K. Mannhardt, H. Engler (Ludwig Neumann), DE-A 3 107 599, *Chem. Abstr.* **1982**, *97*, 198204p.
[24] G. D. Hartmann, L. M. Weinstock, *Synthesis* **1976**, 681.
[25] J. Buschmann, D. Lentz, P. Luger, G. Perpetuo, D. Scharn, S. Willemsen, *Angew. Chem.* **1995**, *107*, 988; *Angew. Chem. Int. Ed. Engl.* **1995**, *34*, 914.
[26] R. Neidlein, *Angew. Chem.* 1964, *76*, 440; *Angew. Chem. Int. Ed. Engl.* **1964**, *3*, 382.
[27] J. Buschmann, T. Bartolmäs, D. Lentz, P. Luger, I. Neubert, M. Röttger, *Angew. Chem.* **1997**, *109*, 2466; *Angew. Chem. Int. Ed. Engl.* **1997**, *36*, 2372.
[28] L. Halonen, I. M. Mills, *J. Mol. Spectrosc.* **1978**, *73*, 494.
[29] D. Christen, K. Ramme, B. Haas, H. Oberhammer, D. Lentz, *J. Chem. Phys.* **1984**, *80*, 4020.
[30] G. Perpetuo, J. Buschmann, P. Luger, D. Lentz, D. Dreissig, *Acta Crystallogr. B* **1999**, *55*, 70–77.
[31] E. F. Pearson, R. A. Cresswell, M. Winnewisser, G. Winnewisser, *Z. Naturforsch. A* **1976**, *31*, 1394.
[32] B. Bak, B. P. van Eijck, C. Kierkegaard, *J. Mol. Struct.* **1973**, *18*, 429.
[33] D. Lentz, D. Preugschat, *Acta Crystallogr. C* **1993**, *49*, 52.
[34] J. Buschmann, S. Kleinhenz, D. Lentz, P. Luger, D. Preugschat, *J. Am. Chem. Soc.* submitted.
[35] T.-A. Chang, M. D. Harmony, S. W. Staley, *J. Mol. Struct.* **1988**, *190*, 17.
[36] M. C. L. Gerry, F. Stroh, M. Winnewisser, *J. Mol. Spectrosc.* **1990**, *140*, 147.
[37] P. Coppens, *X-ray Charge Densities and Chemical Bonding*, Oxford University Press, Oxford, **1997**.
[38] T. Koritsánszky, R. Flaig, D. Zobel, H.-G. Krahne, W. Morgenroth, P. Luger, *Science* **1998**, *279*, 356.
[39] R. Destro, R. Bianchi, C. Gatti, F. Mirati, *Chem. Phys. Lett.* **1991**, *186*, 47.
[40] C. Flensburg, S. Larsen, R. Steward, *J. Phys. Chem.* **1995**, *99*, 10130.
[41] T. Koritsánszky, J. Buschmann, P. Luger, *J. Phys. Chem.* **1996**, *100*, 10547.
[42] R. Flaig, T. Koritsánszky, D. Zobel, P.Luger, *J. Am. Chem. Soc.* **1998**, *120*, 2227–2238.
[43] N. K. Hansen, P. Coppens, *Acta Crystallogr. A* **1978**, *34*, 909.
[44] T. Koritsánszky, S. T. Howard, T. Richter, Z. Su, P. R. Mallinson, N. K. Hansen, XD - a Computer Program Package for Multipole Refinement and Analysis of Electron Densities from Diffraction Data, User Manual, Freie Universität Berlin, **1997**.
[45] E. Clementi, C. Roetti, *Atomic Data and Nuclear Data Tables* **1974**, *14*, 177.
[46] R. F. Stewart, E. R. Davidson, W. T. Simpson, *J. Chem. Phys.* **1965**, *42*, 3175.
[47] C. K. Johnson, ORTEP-Report ORNL-3794 (2nd revision), Oak Ridge, Tennessee, **1970**.

[48] J.-J. Didisheim, D. Schwarzenbach, *Acta. Crystallogr. A* **1987**, *43*, 226.
[49] F. L. Hirshfeld, *Acta Crystallogr. A* **1976**, *32*, 239.
[50] V. Schomaker, K. N. Trueblood, *Acta Crystallogr. B* **1968**, *24*, 63.
[51] M. J. Frisch, G. W. Trucks, H. B. Schlegel, P. M. W. Gill, B. G. Johnson, M. W. Wong, J. B. Foresman, M. A. Robb, M. Head-Gordon, E. S. Replogle, R. Gomperts, J. L. Andres, K. Raghavachari, J. S. Binkley, C. Gonzalez, R. L. Martin, D. J. Fox, D. J. Defrees, J.Baker, J. J. P. Stewart, J. A. Pople, Gaussian 92/DFT, Revision G. 4, Gaussian Inc., Pittsburgh PA, **1993**.
[52] J. Cheeseman, T. A. Keith, R. F. W. Bader, AIMPAC program package, McMaster University, Hamilton, Ontario, **1992**.
[53] R. F. W. Bader, *Atoms in Molecules - A Quantum Theory*, Clarendon Press, Oxford, **1990**.
[54] Z. W. Su, P. Coppens, *Acta Crystallogr. A* **1992**, *48*, 188.
[55] H. Dietrich, H. Dierks, *Meßtechnik (Braunschweig)* **1970**, *78*, 184–186.
[56] K. Obatake, S. Tanisaki, *Phys. Lett. A* **1973**, *44*, 341.
[57] M. T. Dove, A. I. M. Rae, *Faraday Disc. Chem. Soc.* **1980**, *69*, 98.

Received: February 8, 1999 [F1595]

  0947-6539/99/0511-3420 $ 17.50+.50/0